**The effects of environmental parameters on diffuse degassing at Stromboli volcano: Insights from joint monitoring of soil CO2 flux and radon activity**

Laiolo, M., Ranaldi, M., Tarchini, L., Carapezza, M.L., Coppola, D., Ricci, T., Cigolini, C. (2016) The effects of environmental parameters on diffuse degassing at Stromboli volcano: insights from joint monitoring of soil CO2 flux and radon activity. Journal of Volcanology and Geothermal Research, 315, 65–78

http://www.sciencedirect.com/science/article/pii/S0377027316000391

Published on line: Feb 13, 2016

# The effects of environmental parameters on diffuse degassing at Stromboli volcano: insights from joint monitoring of soil $CO_2$ flux and radon activity

Laiolo, M.[1,2*], Ranaldi, M. [3,4], Tarchini, L. [3,4], Carapezza, M.L. [4], Coppola, D. [2], Ricci, T. [4] & Cigolini, C. [2,5]

1 – Dipartimento di Scienze della Terra, Università di Firenze, Via G. La Pira 4, 50121 Firenze, Italy
2 – Dipartimento di Scienze della Terra, Università di Torino, Via Valperga Caluso 35, 10125 Torino, Italy
3 – Dipartimento di Scienze, Università Roma Tre, Largo San L. Murialdo 1, 00146 Roma, Italy
4 – INGV, Sezione Roma 1, Via Vigna Murata 605, 00143 Roma, Italy
5 – NatRisk, Centro Interdipartimentale sui Rischi Naturali in Ambiente Montano e Collinare, Università degli Studi di Torino, Italy

* Corresponding Author - email: marco.laiolo@unito.it

## ABSTRACT

Soil $CO_2$ flux and $^{222}Rn$ activity measurements may positively contribute to the geochemical monitoring of active volcanoes. The influence of several environmental parameters on the gas signals has been substantially demonstrated. Therefore, the implementation of tools capable of removing (or minimizing) the contribution of the atmospheric effects from the acquired timeseries is a challenge in volcano surveillance. Here, we present four years-long continuous monitoring (from April 2007 to September 2011) of radon activity and soil $CO_2$ flux collected on the NE flank of Stromboli volcano. Both gases record higher emissions during fall-winter (up to 2700 $Bq*m^{-3}$ for radon and 750 g $m^{-2}$ $day^{-1}$ for $CO_2$) than during spring-summer seasons. Short-time variations on $^{222}Rn$ activity are modulated by changes in soil humidity (rainfall), and changes in soil $CO_2$ flux that may be ascribed to variations in wind speed and direction. The spectral analyses reveal diurnal and semi-diurnal cycles on both gases, outlining that atmospheric variations are capable to modify the gas release rate from the soil. The long-term soil $CO_2$ flux

shows a slow decreasing trend, not visible in $^{222}Rn$ activity, suggesting a possible difference in the source depth of the of the gases, $CO_2$ being deeper and likely related to degassing at depth of the magma batch involved in the February-April 2007 effusive eruption. To minimize the effect of the environmental parameters on the $^{222}Rn$ concentrations and soil $CO_2$ fluxes, two different statistical treatments were applied: the Multiple Linear Regression (MLR) and the Principal Component Regression (PCR). These approaches allow to quantify the weight of each environmental factor on the two gas species and show a strong influence of some parameters on the gas transfer processes through soils. The residual values of radon and $CO_2$ flux, i.e. the values obtained after correction for the environmental influence, were then compared with the eruptive episodes that occurred at Stromboli during the analysed time span (2007-2011) but no clear correlations emerge between soil gas release and volcanic activity. This is probably due to *i)* the distal location of the monitoring stations with respect to the active craters and to *ii)* the fact that during the investigated period no major eruptive phenomena (paroxysmal explosion, flank eruption) occurred. Comparison of MLR and PCR methods in time-series analysis indicates that MLR can be more easily applied to real time data processing in monitoring of open conduit active volcanoes (like Stromboli) where the transition to an eruptive phase may occur in relatively short times.

## 1 – Introduction

Real-time monitoring of gas release (output and composition) at active volcanoes is useful to forecast changes in volcanic activity. Active volcanoes are characterized by persistent huge gas emissions from craters, fumaroles and also diffusively from soils (Allard et al., 1991; Burton et al., 2013; Inguaggiato et al., 2013) and systematic gas monitoring may help to detect precursory signals of incoming eruptions (e.g., Aiuppa et al., 2009; Padrón et al., 2013). In recent years, this

78 approach was applied at several volcanoes to record geochemical changes during volcanic
79 activity and to investigate their role before, during and after major eruptive episodes (including
80 flank instabilities; e.g., Carapezza et al., 2004 and 2009; Alparone et al. 2005; Cigolini et al.,
81 2005). Another open and debated issue is the role of degassing prior the onset of earthquakes
82 (Toutain and Baubron, 1999; Salazar et al., 2001) and during earthquake-volcano interactions
83 including seismic-volcanic unrest (Cigolini et al., 2007; Padilla et al., 2014).
84 Carbon dioxide, after water, is the most abundant volatile dissolved in magmas and, because of
85 its relatively low solubility in magmatic liquids, it is essentially released at higher depths and
86 before other gas species (Pan et al., 1991, Papale et al., 2006). Notably, measurements of soil
87 $CO_2$ fluxes or $CO_2$ concentrations in volcanic plumes, are critical for detecting degassing
88 processes related to changes in the plumbing system of the volcano.
89 Radon is a noble gas, a daughter decay product of $^{226}Ra$ and belongs to the $^{238}U$ decay chain. Due
90 to its short half-life ($t_{1/2}$= 3.82 days), $^{222}Rn$ can be used as a tracer of both diffuse and localized
91 degassing since it can substantially be measured everywhere. Radon concentrations may be
92 moderate during diffuse degassing, but during fracture opening they may reach extremely high
93 values (higher than $10^6$ Bq/m$^3$, as measured in Stromboli crater area; Cigolini et al., 2013). Its
94 ascent towards the surface is strictly ruled by the mobility of other gas phases, such as $CO_2$ and
95 $H_2O$ defined as "carrier gases" (Gauthier and Condomines, 1999). The joint measurements of
96 soil $CO_2$ flux and $^{222}Rn$ activity have been used to search possible volcanic and seismic
97 precursors (Makario Londoño, 2009), as well as to track fluid migration and outgassing along
98 active faults, fractures or fumaroles (Baubron et al., 2002; Faber et al., 2003; Zimmer and
99 Erzinger, 2003). Moreover, combined surveys of $^{222}Rn$, $^{220}Rn$ and $CO_2$ give us a clue to
100 discriminate distinct gas sources (i.e. rock fracturing, hydrothermal, magmatic) (Giammanco et

al., 2007; Siniscalchi et al., 2010) and, to track the evolution of a volcanic unrest phase (Padilla et al., 2013).

Continuous and automatic measurements substantially increase the possibility to identify precursory signals, since the data are easily collected, transferred and processed in near real-time (Brusca et al., 2004; Viveiros et al., 2008; Cigolini et al., 2009; Carapezza et al., 2009). Environmental parameters are critical in modulating gas release from soils, including radon and $CO_2$ (Pinault and Baubron, 1996; Carapezza and Granieri, 2004; Pérez et al., 2007; Cigolini et al., 2009) and their effects must be considered during continuous geochemical monitoring.

In this respect, a promising challenge is to establish a fully-automated data processing able to minimize the effects of environmental factors on the acquired data. In this way, data obtained by the geochemical monitoring networks can be easily transferred to the authority responsible of volcano surveillance. The statistical treatment or the spectral analysis of the data are the mostly used methods to recognize and remove the contribution of the atmospheric factors (e.g. Carapezza et al., 2009; Laiolo et al., 2012; Rinaldi et al., 2012; Silva et al., 2015; Viveiros et al., 2008; 2014). Particularly, the spectral analysis may be positively applied to recognize diurnal to seasonal cycles and to investigate the processes ruling the release of gases from soils (Rinaldi et al., 2012; Martin-Luis et al., 2015).

Radon concentrations can be diluted by major fluxes of $CO_2$ and water vapor (e.g., Giammanco et al., 2007; Siniscalchi et al., 2010). Recently, Girault et al. (2014) and Girault and Perrier (2014) have shown, at the Syabru-Bensi hydrothermal system (Central Nepal), that radon is generated from a shallow source (a rock thickness of 100 m is sufficient to account for the observed radon discharge) and incorporated into upraising $CO_2$. In active volcanoes radon can be carried to the surface from great depths along major faults. Cigolini et al. (2013) have shown that

high radon emissions can be related to the ascent of $CO_2$-bearing hot fluids along the fractures (200-300 m deep) surrounding the crater rim of Stromboli volcano (at about 700-720 m a.s.l.) and well correlate with the estimated depth of the source region of VLP events (e.g., (Chouet et al., 1997; Marchetti and Ripepe, 2005). Previous investigations have shown that $CO_2$ fluxes and $^{222}Rn$ concentrations at Stromboli are within the range of those measured in other open-conduit active volcanoes (Cigolini et al., 2013; Inguaggiato et al., 2013).

In this paper, we present four years of continuous monitoring of $^{222}Rn$ activity and soil $CO_2$ flux collected by two automatic stations located on the north-eastern upper flank of Stromboli Island (Fig. 1). The measurement sites have been chosen in the light of previous surveys: anomalous radon values were recorded in this site during periods of sustained volcanic activity and before, during and after the paroxysmal explosion of March 15, 2007 (Cigolini et al., 2013). Similarly, systematic measurements of soil $CO_2$ flux revealed anomalous degassing areas on the volcano slopes and this site has been identified as a potential target for continuous monitoring (Carapezza et al., 2009).

## 2 – Stromboli volcano

Stromboli is the north-easternmost island of the Aeolian archipelago and reaches an elevation of 924 m a.s.l. (Fig. 1). It is a composite stratovolcano consisting of lava flows alternated with abundant tephra deposits. The emerged part of the volcanic edifice was built in the last 100 ky (Francalanci et al., 1989; Hornig-Kjiarsgaard et al., 1993). The morphology of the island results from periods of extrusive growth alternated to lateral collapses, in turn related to dyke intrusions, magma upwelling and regional tectonics (Tibaldi, 2003 and 2004; Corazzato et al., 2008). The volcano is well known for its typical persistent explosive activity called Strombolian, that started

147 approximately 2 ky ago (Rosi et al., 2000; Arrighi et al., 2004). Strombolian activity is
148 characterised by continuous degassing with the emission, on average every 15-20 minutes, of
149 juvenile material (glowing scoriae, lapilli and ash) ejected from the active vents located within
150 the crater terrace at ~700 m. a.s.l. This mild explosive activity is episodically interrupted by lava
151 flows, major and paroxysmal explosions (Barberi et al., 1993 and 2009) that can be accompanied
152 by flank failure and collapses, which may also generate tsunamis, like in 1930 and recently in
153 December 2002 (Tinti et al., 2006). Paroxysmal events, such as the ones occurred on April 5,
154 2003 and March 15, 2007, are the most violent volcanic explosions of Stromboli and are
155 characterized by the ejection of the so-called "golden pumices" (nearly aphyric, phenocrysts < 10
156 vol%, highly vesicular > 50 vol%, low viscosity K-basaltic pumiceous materials; Métrich et al.,
157 2005 and 2010). These ejecta are generally mixed with degassed scorias (the latter also ejected
158 during the typically mild Strombolian activity) and with ballistic solid blocks. The $CO_2$ and $H_2O$
159 contents measured in primitive melt inclusions, found within forsteritic olivines of the golden
160 pumices, indicate that these materials represent the undegassed magma residing in the deeper
161 part of the Stromboli plumbing system (Bertagnini et al., 2003; Francalanci et al., 2004; Métrich
162 et al., 2005; Cigolini et al., 2008; 2014).
163 Soon after the 2002-2003 effusive event, a great improvement of the monitoring system was
164 undertaken under the coordination of the Italian Civil Protection Department. This advance on
165 ground-based monitoring allowed the scientific community to acquire a great amount of
166 geophysical, geochemical and geodetic data during the most recent effusive episodes, as well as
167 during the span of time characterized by low to high explosive activity (cf. Barberi et al., 2009;
168 Ripepe et al., 2009; Calvari et al., 2014; Rizzo et al., 2014). Recent investigations have also

shown that within the latter years there was an increase in the radiative heat power associated to several minor lava overflows within the summit area (Coppola et al., 2012; Calvari et al., 2014). Geochemical monitoring at Stromboli has involved the following activities: soil radon concentration (Cigolini et al., 2009 and 2013), soil $CO_2$ flux (Carapezza et al., 2004 and 2009; Federico et al., 2008; Rizzo et al., 2009 and 2014), $SO_2$ plume measurements by COSPEC (Burton et al., 2009), continuous measurements of $CO_2/SO_2$ ratios within the volcanic plume (Aiuppa et al., 2009 and 2011). These methods were tested to eventually forecast paroxysms and major explosions; in addition, the continuous monitoring of low-temperature fumaroles was useful to detect short-time changes in volcanic activity (Madonia and Fiordilino, 2013). The extension and structure of the complex hydrothermal system of the volcano has been investigated by multidisciplinary studies (involving electrical resistivity, soil $CO_2$ concentration, temperature and self-potential measurements; Finizola et al., 2006 and 2009; Revil et al., 2011). Geochemical studies on the geothermal aquifer at the periphery of the volcano is an additional tool to detect precursory signals of an impending eruption (Carapezza et al., 2004; Capasso et al., 2005).

## 3 – Methods and Techniques

Preliminary radon and carbon dioxide surveys were conducted to find the most appropriate sites for continuous monitoring. A network of 21 radon stations has been operative at Stromboli since 2002 (Cigolini et al., 2005; 2009; 2013). Systematic measurements were undertaken by using LR115 track-etches alpha-detectors exposed from two to six weeks (Bonetti et al., 1991), in order to obtain continuous time series on $^{222}Rn$ emissions. Additionally, periodic short-term measurements has been performed by means of EPERM® electretes (Kotrappa et al., 1993) that

allowed to better correlate radon emissions with the variations of volcanic activity (Cigolini et al., 2005 and 2007). These periodic measurements demonstrated that diffuse degassing occurs at Stromboli mainly along the main structural discontinuities. After the February-April 2007 effusive-explosive event, a real-time station for radon measurements was first installed at 520 m a.s.l. at Liscione, on the northeastern side of the cone (see Fig. 1 and Fig. 2a). Similarly, a soil $CO_2$ flux survey first outlined the main sectors of gas emanation (Carapezza and Federico, 2000) and two automatic soil $CO_2$ flux stations (and environmental parameters) were installed at Stromboli: one at the summit (Pizzo sopra La Fossa) in 1999, and the second one near the sea-shore in 2001 (Pizzillo). In the following years, $CO_2$ soil concentration surveys, within the crater terrace and surrounding areas, were performed to identify the sectors of major degassing and higher hydrothermal activity (Finizola et al., 2002 and 2003). Furthermore, Carapezza et al. (2009) performed a wide detailed survey of soil $CO_2$ flux on the island and sectors of anomalous degassing were detected. Therefore, two soil $CO_2$ flux and multiparametric fully-automated stations were installed along the ENE flank of the volcano (respectively at Rina Grande and Nel Cannestrà) where anomalous gas emissions were found (Carapezza et al., 2009) (Fig. 2b).

Dataset analysed in this paper refer to the $^{222}Rn$ and $CO_2$ measurements acquired by fully automated stations located in the Nel Cannestrà sector (see Fig. 1 and 2). The area is confined between two major structural discontinuities (the N40°E fault, and the N60°E fault) that cross-cut the north-eastern sector of Stromboli. These automated stations consist of two units, one for measuring the isotope of the radon progeny (together with soil temperature and atmospheric pressure) and the other for measuring soil $CO_2$ flux (by accumulation chamber) together with environmental parameters (atmospheric temperature, humidity and pressure; soil humidity and temperature; wind direction and horizontal speed). The radon unit provides near real-time

measurements of $^{222}$Rn concentrations (by using a DOSEMan, Sarad Gmbh, Germany) connected to an electronic board able to acquire and transfer the collected data to a radio-modem that sends, by means of a directional antenna, the signal to the COA volcano observatory. The station acquires data every 30 minutes and the radon concentration and soil temperature are measured at 1 m depth. The DOSEMan radonmeter measures α-particles within a 4.5-10 MeV energy window, including both $^{218}$Po and $^{214}$Po peaks (Gründel and Postendörfer, 2003). An exhaustive description of the radon dosimeter and of the real-time $^{222}$Rn station can be found in Cigolini et al. (2009) and Laiolo et al. (2012). Soil $CO_2$ flux and environmental parameters are measured hourly with a fully equipped automated station produced by West Systems (see Carapezza et al., 2009 for method description). Soil temperature and humidity are measured at 50 cm depth; air $CO_2$ concentration is measured 30 cm above the soil/air interface (Carapezza et al., 2009). Data are stored on a non-volatile memory and can be retrieved by means of a telemetry system at the volcano observatory (COA, see Fig. 1). The main technical characteristics of the sensors used in both stations are reported in the supplementary materials (Table S1).

The timespan investigated in this work (April 2007 - September 2011) matches the period in which both instrumentations were mostly operative. In fact, the $^{222}$Rn station was installed in early April 2007 and is still operative whereas the automated $CO_2$ flux station, installed in mid March 2007, was dismissed in late September 2011.

## 4 – Results

### *4.1 – Time series of soil $CO_2$ flux and $^{222}$Rn activity*

236 The overall behaviour of the $CO_2$ and $^{222}Rn$ signals is somehow similar in the first two years:
237 they both show bell-shaped profiles, strongly ruled by seasonal trend, that reach their lower and
238 stable values during summer and the higher values, with a wider variation range, in winter. A
239 similar behaviour is observed also in multi-modal distributions (see histograms in Fig. 3). Both
240 trends display several marked spikes within each time series (Fig. 3a and 3b) and numerous
241 peaks of the two gases are essentially concordant. In the last two years, soil $CO_2$ flux shows a
242 decreasing trend, whereas radon activity maintains nearly the same annual average, or simply
243 increase (see Table 1).
244 Compared with other active volcanic areas, radon shows relatively low concentration (cf.
245 Cigolini et al., 2013 and references therein). Values are essentially below 2000 Bq/m$^3$ for a large
246 part of the year and may exhibit a short-term variability; the average activity in the four years is
247 around 2000 Bq/m$^3$ with a standard deviation of 1200 Bq/m$^3$ (Table 1). During winter
248 (November-February), radon typically exhibits higher average values (Fig. 3a) with peaks up to
249 7900 Bq/m$^3$. We remind that the $^{222}Rn$ activity in the summit area, close to the active vents,
250 shows significantly higher average values reaching 12,500 Bq/m$^3$ (± 4,200; Laiolo et al., 2012;
251 Cigolini et al., 2013).
252 Radon seasonal minima refer to late spring-summer periods (March-October) with average
253 values of ~1200 Bq/m$^3$ and hourly minima close to 200 Bq/m$^3$. The $^{222}Rn$ long-term stability on
254 low values seems closely related to the absence of marked weather changes during this season.
255 The time-series of environmental parameters are shown in Fig. 4; a preliminary analysis of their
256 effects, supported by the correlation coefficients (Table 2), shows that both the $^{222}Rn$ and $CO_2$
257 signals are inversely correlated to soil and air temperature, and positively correlated (especially
258 radon) to soil humidity, in turn depending on rainfall. It is interesting to point out that sudden

variations in radon concentrations normally occur within few hours of continuous raining and/or temperature drops. A similar phenomenon has been observed at Furnas volcano (Azores archipelago) during continuous monitoring of $CO_2$ flux (Viveiros et al., 2008) and radon activity (Silva et al., 2015).

The relation between temperature and $^{222}Rn$ activity is ascribed to the local thermal gradient (between soil and air temperatures) that affects the efficiency of the in-soil convective cells and, consequently, the migration of gas toward the surface (Mogro-Campero and Fleisher, 1977; Cigolini et al., 2001). Therefore, a marked difference between soil and air temperatures, typical of the fall-winter season, causes an increase in the measured radon activities. The entire dataset shows a clear positive correlation (R= 0.74; Table 2) between soil moisture and radon emissions; indeed, an increase in soil moisture may increase the $^{222}Rn$ emanation coefficient (i.e. exhalation rate) by one order of magnitude (Nazaroff, 1992; Sakoda et al., 2010; Girault and Perrier, 2012). However, to evaluate the relation between $^{222}Rn$ activity and soil humidity, we have also to consider the confinement of the box containing the radon detector. The device is placed in an impermeable polycarbonate case (permeable to $^{222}Rn$ but not to water) at a depth of about 1 m. Thus, if the soil matrix surrounding the case is affected by water saturation, the preferential pathway for radon migration will follow the interface soil-bottom of the case, leading to an increase in α decay counts. Another possibility is that, during a rainfall episode, only the higher portions of soil (down to about 10-30 cm) undergo water saturation that, in turn, temporarily inhibits the free motion of the radon particles toward the surface. Consequently, radon will preferentially be confined at lower levels (i.e., where water content is low or absent) so that decay counts will be drastically higher in the portion of soil where the case (containing the detector) is inserted. As the relation between soil humidity and radon activity essentially depends

from soil permeability, the observed behaviour can be inhomogeneous over a given sector of the volcano (Perrier et al., 2009).

Soil $CO_2$ flux measurements acquired by the automatic station started on mid-March 2007. The four years average value for $CO_2$ flux is ~600 (±643) g $m^{-2}$ day-1 with a rather high standard deviation (as for radon) (Table 1). The maximum values were reached in January 2008 with fluxes slightly exceeding 7000 g $m^{-2}$ $day^{-1}$. As already observed for $^{222}Rn$ activity, minima in soil $CO_2$ fluxes occur during summer-early fall when values well below 100 g $m^{-2}$ $day^{-1}$ were recorded. A similar trend outlines that the variation of the local thermal gradient is capable to affect also the $CO_2$ flux from the soil (Viveiros et al., 2014).

Surprisingly, there is a noticeable correlation between soil $CO_2$ flux and wind, both speed (positive) and direction (negative) (Table 2). In Fig. 5 it is clear how winds blowing toward SE at speed > 8 m/s are able to produce an efficient gas escape from the soil, causing an increase of the $CO_2$ flux. Such a behaviour is mainly related to a Venturi effect due to a local condition of the Nel Cannestrà station site, that cannot be extrapolated to other sectors of the volcano, considering that it was not observed in the Rina Grande station (see Fig. 2b for location) (Carapezza et al., 2009).

It is interesting to note that the four years-long dataset exhibits a declining long-term trend (Fig. 3b and annual average in Table 1) which can be likely viewed as a decreasing supply of $CO_2$-rich magma from the deeper to the upper plumbing system. This hypothesis is supported by the long-term trend observed in the $CO_2$ emissions from the plume, retrieved by combining $CO_2/SO_2$ ratios and $SO_2$ flux measurements (Aiuppa et al., 2011). The decreasing trend of the soil $CO_2$ flux, marked by the annual average shifting from 920 (in 2007-2008) to 330 g $m^{-2}$ $day^{-1}$ (in 2010-

2011), is not evident in the radon long-term signals that instead show a slight increase from 1777 to 2264 $Bq/m^3$ in annual averages (see straight lines in Fig. 3a and 3b, respectively and Table 1).

### *4.2 – Short-term periodicity and long-term trends*

In order to identify diurnal and semidiurnal cycles affecting the gas signals, we performed a spectral analysis (Power Spectral Density) over a one year subset of data (sample time = 1 hour), using the method suggested by Viveiros et al. (2014). The analysis identified the 12h and the 24h frequency peaks in both $CO_2$ flux and $^{222}Rn$ activity (Fig. 6), confirming previous findings (Perrier et al., 2009 and 2012; Rinaldi et al., 2012). In our case, the $^{222}Rn$ signal seems to be modulated by temperature and barometric changes, although we do not exclude that this periodicity could be related with solar tides (e.g., Steinitz et al. 2011). On the other hand, the soil $CO_2$ flux reveals a main 12h period. It is worth noting that such a behaviour slightly differs from previous results suggesting a major influence of temperature rather than pressure (Rinaldi et al., 2012).

By analysing the long-time series of soil $CO_2$ flux and $^{222}Rn$ activity, we performed a calculation of the mean value of the whole data for each specific day of the year and the same computation was carried out also on soil and air temperature data. The emerging annual trend (see Fig. 7a, b) highlights the inverse relation between temperature and soil gas release, as well as an apparent correlation between the two gas species. Overall, we observe a 100% increment of the mean values comparing the spring-summer with the fall-winter period. It is also evident that the most significant day-by-day variations occur during the fall and spring season, when the likelihood of drastic atmospheric changes (i.e. heavy rainfall or windstorm) is higher than during summer.

326 The long-period behaviour is ruled by soil and air temperature (i.e. thermal gradient), whereas
327 short-time oscillations are modulated by soil humidity (e.g., rainy events) and wind conditions
328 (speed and direction), respectively. The correlation coefficients (R) shown in Table 2, allow to
329 better assess the effect of the environmental parameters that actively modulate the trends of $^{222}Rn$
330 activity and soil $CO_2$ flux.
331

332 ***4.3 – Variation of the correlation coefficients***

333 The seasonal variations of average correlation coefficients of the main environmental parameters
334 with $^{222}Rn$ activity and soil $CO_2$ flux are reported in Fig. 8, where seasons are gathered and
335 simply subdivided in spring-summer and fall-winter subsets. It can be seen that the correlation
336 coefficients are not so stable throughout the investigated time span, but appear slightly
337 modulated by seasonal effects. For example, both soil $CO_2$ flux and radon activity display a more
338 distinctive negative correlation with air and soil temperatures during the spring-summer subsets.
339 This behaviour is likely due to the lack of drastic variations in weather conditions during the
340 "dry" season at Stromboli Island. Hence, the correlation between temperature and gas flux and
341 concentration is not perturbed by other atmospheric factors (e.g. soil humidity). Correlation
342 coefficients seem somewhat different in the first subset (spring-summer 2007) compared to all
343 the others; this subset (grey field in Fig. 8) was obtained just after the March 15, 2007 explosive
344 paroxysm when the effects of environmental conditions on degassing dynamics, even in
345 relatively distal areas, seem somehow weaker. In April-June 2007 the lava effusion ceased and
346 the Strombolian activity was not resumed, or more precisely, the source of explosions was too
347 deep to allow glowing scoriae to reach the crater surface. In this time span, there was still a

348 remarkable degassing rate at the craters from a relatively deep-seated magma level (Aiuppa et
349 al., 2009; Barberi et al., 2009).

350 ***4.4 – Statistical treatment***

351 Two different statistical methods have been applied on the raw dataset (sample time = 1 hour) of
352 soil $CO_2$ flux and $^{222}Rn$ concentration in order to identify and remove the effects due to
353 environmental parameters.

354 *4.4.1 - Multiple Linear Regression Statistics (MLR)*

355 The datasets of radon concentration, soil $CO_2$ flux and environmental parameters have been
356 analysed by the Multiple Linear Regression (MLR) which is a simple and largely applied method
357 used to identify the contributions of several independent variables and model the fluctuations
358 observed in the investigated signal. The analysis has been performed to predict the values of a
359 dependent variable (Y) given a set of predictor variables ($X_1$, $X_2$, …., $X_n$). The relationship
360 between the dependent variable (Y*calc*) and the predicted variables is expressed as

361 $$Y_{calc} = Y_0 + b_1X_1 + b_2X_2 + \ldots + b_nX_n \quad (1)$$

362 $Y_0$ is the intercept, $X_n$ are the acquired variables and $b_n$ the calculated regression coefficients
363 (Granieri et al., 2003; Hernandez et al., 2004; and references therein). In order to simplify and
364 reduce the number of predictor variables, MLR takes into account only the factors that are more
365 correlated (positively or negatively) with $CO_2$ flux and $^{222}Rn$ activity (Table 3). By considering
366 previous research, we selected only the environmental factors (i.e. independent variables)
367 causing an increment of the $R^2$ greater or equal to 1% (Viveiros et al., 2008; Silva et al., 2015).
368 Particularly, soil and air temperature were indicated by the regression for both gas species,

369 together with wind speed and direction for $CO_2$ and soil humidity for $^{222}Rn$. In Table 3 we report
370 the main parameters for both gases by the MLR analysis.
371 Results show that the atmospheric variables taken into account for this analysis are able to
372 predict 45% and 51% (R= 0.67 and R= 0.71) of the variations observed in soil $CO_2$ flux and
373 $^{222}Rn$ concentration, respectively. Moreover, soil $CO_2$ flux and $^{222}Rn$ values show low
374 dispersions, as respectively the 4.8% and 4.0% of the computed residuals exceed the average ±2
375 standard deviation range. Predicted values by MLR both for radon concentration and soil $CO_2$
376 flux, together with the observed values and the calculated residuals, are plotted in Fig. 9a onto
377 the recorded time series. By looking at the residuals, it can be seen that *i)* the bell shape of the
378 $CO_2$ flux is smoothed due to the removal of the seasonal trend but it still persists for radon, and
379 *ii)* the residuals of both gases show peaks and major fluctuations that obviously cannot be related
380 to environmental variations. Moreover, in both cases the signals are still characterised by noisy
381 components (as reported by Laiolo et al., 2012 and Viveiros et al., 2014).
382 This statistical approach has been used at different volcanoes in the attempt to detect short-term
383 variations in volcanic activity (e.g. major explosions at Stromboli; Laiolo et al., 2012), as well as
384 the effects of seismic sequences (due to stress/strain structural changes) on the shallow part of a
385 volcanic edifice (e.g., Masaya as analysed by Padilla et al., 2014).

386 *4.4.2 - Principal Component Regression (PCR)*

387 The second statistical treatment applied to $^{222}Rn$ activity, soil $CO_2$ flux and environmental
388 parameters is the Principal Component Regression (PCR). This method differs from the previous
389 one in how predictors are treated: first, a factor analysis is performed on the environmental
390 dataset (*X*); then a forward step-wise linear regression of measured soil $CO_2$ flux and radon
391 activity (*Y*) is performed on the estimated factors. The goal of this approach is firstly to obtain a

392 reduction in the *X* data set in a way that maintains the maximum amount of information (i.e.
393 largest possible variance), and secondly to perform regression of *Y* on orthogonal (uncorrelated)
394 components. The aim is to ensure that highly correlated principal components are not overlooked
395 (Vandeginste et al., 1998).
396 We performed factor analysis on two separate datasets because the radon station measures soil
397 temperature and air pressure, whereas soil $CO_2$ flux station also measures air and soil humidity,
398 wind speed and direction. Therefore, we created one dataset for radon with soil temperature and
399 atmospheric pressure measured at the radon station and added the other variables measured at the
400 $CO_2$ station**.** The factor analysis of the two datasets shows that three eigenvalues are higher than
401 1.0 and these three factors can explain the 73% of the total variance (Table 4). In the second step,
402 we performed forward step-wise regressions of $^{222}Rn$ concentration and soil $CO_2$ flux on the first
403 three factors. We obtained two theoretical models which explain the 25% and the 47% (R= 0.50
404 and R= 0.68) respectively of the soil $CO_2$ flux and $^{222}Rn$ concentration measurements variance
405 (Table 4b). As in the MLR model, residual values show low dispersion, being less than 5% the
406 portion of the data that exceeds the mean $\pm 2\sigma$ range (4.11% and 4.89% for $CO_2$ and $^{222}Rn$,
407 respectively). The time series of observed, predicted and residual values of radon concentration
408 and soil $CO_2$ flux are reported in Fig. 9b. An overall comparison of the latter with Fig. 9a shows
409 that the two statistical treatments provide basically the same results.

410 **5 – DISCUSSION**

411 For $^{222}Rn$, the applied statistical methods indicate nearly the same percentage of data attributed
412 to environmental variations, whereas the predicted soil $CO_2$ flux values vary from 45% in MLR
413 to 25% in PCR. The residual computed values are related to processes that are likely related to

414 the volcanic system and occur either within the shallow hydrothermal aquifer or in the deep
415 magmatic plumbing system. It can be noted that the radon treatments provide many significant
416 negative residual values $\leq -2\sigma$, whereas only one negative residual is recorded for soil $CO_2$ flux
417 (see Fig. 10). This indicates that, according to the statistical treatments, the measured radon
418 concentrations are frequently lower than those calculated by filtering the effects of the
419 environmental factors. We explain the high fluctuations showed by the residuals of radon signal
420 with the relative low sensitivity of the radon dosimeter (Table S1) when settled with a high
421 sampling rate (1 hour) in areas characterised by general low emissions (< 2000 $Bq/m^3$). In fact,
422 such a noisy signal was not observed in the datasets acquired where the radon emissions are
423 higher (Laiolo et al., 2012). Moreover, a trend characterised by positive and negative fluctuations
424 in the calculated $^{222}Rn$ residual values, has been already observed in a non-volcanic area
425 (Hayashi et al., 2015).
426 The residual time series (Fig. 9) retrieved for soil $CO_2$ flux shows in both treatments a decreasing
427 trend for the first two years (visible also in the raw data) followed by a nearly steady-state signal
428 close or below the zero value. This behaviour supports the hypothesis that the supply of $CO_2$-rich
429 magma from the deep plumbing system (that started before the 2007 eruption, Aiuppa et al.,
430 2011), besides increasing $CO_2$ emission in the gas plume itself, induced also a higher $CO_2$ flux in
431 more distal zones, which lasted for nearly two years.
432 Comparison of the standard residuals (both by PCR and MLR) for $CO_2$ soil flux and $^{222}Rn$
433 activity versus time (Fig. 10) shows that in the initial two years of monitoring (up to May 2009)
434 the two gases display a similar behaviour with nearly synchronous alternation of periods with
435 anomalous emissions and periods with few or no anomalies (such as the summer of 2007 and

436 2008). In the last two years considered, only radon shows frequent positive anomalies whereas
437 anomalous $CO_2$ flux values are only rarely recorded.
438 The comparison between the two statistical treatments suggests that MLR is more adequate for
439 getting the quick results needed in near-real time volcano monitoring, whereas PCR ensures a
440 more accurate estimate of data, which might be eventually useful for a more accurate post-
441 process analysis and for a more reliable monitoring.
442 In order to assess the reliability of radon activity and soil $CO_2$ flux, measured in the distal site of
443 Liscione/Nel Cannestrà, as possible precursors of major changes in the volcanic activity, the
444 residuals time-series obtained by PCR and MLR and exceeding $2\sigma$, have been compared with the
445 main volcanic and seismic events occurred at Stromboli in the same time span (Fig. 10).
446 The 4.5 years of gas monitoring (April 2007 - September 2011) represent a phase of ordinary
447 volcanic activity of Stromboli. In this period, twelve major explosions, four minor lava
448 overflows and a local earthquake (with $M_L$= 2.2) were recorded at Stromboli by the INGV
449 monitoring system (Calvari et al., 2014). No explosive paroxysm or effusive eruption occurred.
450 There is no clear correlation between our data and the recorded volcanic events, but some useful
451 considerations can be done.
452 From Fig. 10, it can be seen that in the first two years (following the 2007 explosive and effusive
453 eruptive phase), frequent and high $CO_2$ flux and $^{222}Rn$ anomalies were recorded in coincidence
454 with some anomalous volcanic episodes. Actually, the high number of positive residuals, from
455 October 2007 to June 2008 and from November 2008 to May 2009, coincide with five major
456 explosions and one lava overflow. During the 2007, 2008 and 2009 summers, neither major
457 explosion/lava overflow nor residual $CO_2$ flux peaks were recorded (very few for radon, apart
458 from 2009 summer when data were not available). In summer 2010, two major explosions

occurred in a period of no anomalous gas release. During December 2010 – February 2011 a major explosion and two lava overflows occurred in concurrence with isolated peaks of $CO_2$ flux and during a phase of anomalous $^{222}Rn$ emission. Also the most-recent lava overflow in September 2011 coincided with an anomalous radon activity value.

Conversely, we have to consider that the eruptive events that occurred in the above time span seem to be connected to minor changes associated to the dynamics of the upper part of the conduit (e.g., Barberi et al., 1993 and 2009) without any involvement of the deep seated gas-rich magma pockets (typically occurring during major effusive-explosive cycles of Stromboli volcano, such as those of 2002-2003 and 2007).

## 6 - CONCLUSIONS

The presented data refer to more than four years of soil gas measurements ($^{222}Rn$ concentration and soil $CO_2$ flux) at relatively distal sites from the active vents (Liscione and Nel Cannestrà sites on the NE flank of Stromboli, Fig. 1) during a the time-span (April 2007–September 2011) without major lava effusions and paroxysmal explosions.

The long-time averages for $CO_2$ flux and radon concentration exhibit relatively low values (585 g $m^{-2}$ $day^{-1}$ and 2050 $Bq/m^3$, respectively) when compared to those measured at the summit crater area (Carapezza et al., 2009; Cigolini et al., 2009 and 2013). This means that the advective processes, able to enhance the gas release from soil, are considerably reduced moving away from the crater area. The long term declining trend observed for the soil $CO_2$ flux (Fig. 9 and Table 1) suggests that the large supply of $CO_2$-rich magma associated with the 2007 eruption (and invoked to explain the exceptional $CO_2$ emissions from the plume; Aiuppa et al., 2009 and 2011)

affected also the soil gas release in relatively distal areas. So, as already stressed by De Gregorio et al. (2014) for Etna volcano, the soil $CO_2$ flux measurements represent a key tool to infer the magma supply dynamics and to evaluate the local degassing regime. Furthermore, the combination of soil $CO_2$ flux and $^{222}Rn$ concentration measurements can better constrain the gas source in relation to changes in volcanic activity (Faber et al., 2003; Perez et al., 2007; Padilla et al., 2013). In the last two years (2010 - 2011) of our monitoring, anomalous radon concentrations have been frequently recorded in periods with rare or absent soil $CO_2$ flux anomalies; this likely indicates a different source for the two gases, deeper for $CO_2$ and somehow shallower for radon.

The four years monitoring of both gas species at Stromboli provided the opportunity of better decoding how gaseous transfer toward the surface is ruled by environmental changes. Our data show that both gases are affected by seasonal temperature variations giving to the time series a bell shaped profile. In particular, higher emissions occur during fall-winter, because fluid convection is promoted by the higher soil-air temperature gradient. Conversely, during summer, this gradient is reversed and near-surface convection is inhibited. Moreover, soil $CO_2$ flux is locally influenced by wind (>8 m/s in the SE sector), while radon activity by soil humidity.

In summary, the decreasing surface temperature, eventually coupled with increases in soil moisture seems the main factor that controls the variations of radon emissions. The effect of soil humidity on radon activity probably reflects the adopted measurement techniques. In fact the radon measurements at 1 m depth are likely affected by soil humidity (particularly during the raining falls) which affects the radon diffusion and exhalation rates (i.e., Papachristodoulou et al., 2007).

We have shown that the influence of environmental parameters on gaseous time series can be minimised by means of linear statistics to better evaluate possible variations related to changes in

volcanic activity. The statistical methods presented in this paper can be adopted for different purposes; the Principal Component Regression (i.e. Factor Analysis) appears the more suitable for an accurate analysis of large datasets following major changes in volcanic activity (post-event data processing): in fact, the application of this method carefully evaluates the contribution of each independent factor by means of precise cross correlations. Conversely, Multiple Linear Regression analysis can be more quickly and easily applied to a nearly real-time soil gas monitoring useful in volcano surveillance since it gives us the opportunity to efficiently track anomalous gas concentrations, or fluxes, that are not related to environmental factors. We thus emphasize that the reported datasets represent a rather unique case, at the global scale as well, of geochemical and environmental data acquired in a very active volcanic area for such a long time. The monitored area represents an anomalous degassing zone (Carapezza et al., 2009; Cigolini et al., 2013) and our results show that a multiparametric geochemical monitoring may play a key role in decoding precursory signals related to major changes of Stromboli volcanic activity.

## Acknowledgments

This research was partly funded by Italian Ministry of University and Research (MIUR) and by University of Torino-Fondazione Compagnia di San Paolo. Additional funds were provided by the Italian "Presidenza del Consiglio dei Ministri – Dipartimento della Protezione Civile (DPC)" through the DEVnet Project (a cooperative program between the Departments of Earth Sciences of the University of Torino and the University of Florence) and through the "Potenziamento Monitoraggio Stromboli" project. Additional funds for improving our computing hardware were provided by Fondazione Cassa di Risparmio di Torino. The paper benefited of the suggestions of the F. Viveiros and an anonymous reviewer.

## References


Aiuppa, A., Federico, C., Giudice, G., Giuffrida, G., Guida, R., Gurrieri, S., Liuzzo, M., Moretti, R., Papale, P., 2009. The 2007 eruption of Stromboli volcano: insights from real-time measurement of the volcanic gas plume $CO_2/SO_2$ ratio. J. Volcanol. Geotherm. Res. 182 (3-4), 221–230.

Aiuppa, A., Burton, M., Allard, P., Caltabiano, T., Giudice, G., Gurrieri, S., Liuzzo, M., Salerno, G., 2011. First observational evidence for the $CO_2$-driven origin of Stromboli's major explosions. Solid Earth 2 (2), 135-142.

Allard, P., Carbonelle, J., Dajlevic, D., Le Bronec, J., Morel, P., Robe, M.C., Maurenas, J.M., Faivre-Pierret, R., Martin, D., Sabroux, J.C., Zettwoog, P., 1991. Eruptive and diffuse emissions of $CO_2$ from Mount Etna. Nature 35, 387–391.

Alparone, S., Behncke, B., Giammanco, S., Neri, M., Privitera, E., 2005. Paroxysmal summit activity at Mt.Etna (Italy) monitored through continuous soil radon measurements. Geophys. Res. Lett. 32 (16). doi: 10.1029/2005GL023352.

Arrighi, S., Rosi, M., Tanguy, J., Courtillot, V., 2004. Recent eruptive history of Stromboli (Aeolian Islands, Italy) determined from high-accuracy archeomagnetic dating. Geophys. Res. Lett. 31. doi: 10.1029/2004GL020627.

Baldi, P., Fabris, M., Marsella, M., Monticelli, R. 2005. Monitoring the morphological evolution of the Sciara del Fuoco during the 2002–2003 Stromboli eruption using multi-temporal photogrammetry. ISPRS J. Photogramm. Remote Sens. 59 (4), 199–211.

548 Barberi, F., Rosi, M., Sodi, A., 1993. Volcanic hazard assessment at Stromboli based on review
549 of historical data. Acta Vulcanol. 3, 173-187.
550 Barberi, F., Civetta, L., Rosi, M., Scandone, R., 2009. Chronology of the 2007 eruption of
551 Stromboli and the activity of the Scientific Synthesis Group. J. Volcanol. Geotherm. Res.
552 182 (3-4), 123-130.
553 Baubron, J.C., Rigo, A., Toutain, J.P., 2002: Soil gas profiles as a tool to characterize active
554 tectonic areas: the Jaut Pass example (Pyrenees, France). Earth. Planet. Sci. Lett., 196, 69–
555 81.
556 Bertagnini, A., Métrich, N., Landi, P., Rosi, M., 2003. Stromboli volcano (Aeolian Archipelago,
557 Italy): An open window on the deep-feeding system of a steady state basaltic volcano. J.
558 Geophys. Res. B Solid Earth 108 (7), ECV 4-1–4-15.
559 Bonetti, R., Capra, L., Chiesa, C., Guglielmetti, A., Migliorini, C., 1991. Energy response of
560 LR115 cellulose nitrate to α-particle beams. Nucl. Radiat. Measur. 18, 321-338.
561 Brusca, L., Inguaggiato, S., Longo, M., Madonia, P., Maugeri, R., 2004. The 2002–2003
562 eruption of Stromboli (Italy): Evaluation of the volcanic activity by means of continuous
563 monitoring of soil temperature, $CO_2$ flux, and meteorological parameters. Geochem.
564 Geophys. Geosyst. 5 (12), Q12001. doi:10.1029/2004GC000732.
565 Burton, M.R., Caltabiano, T., Murè, F., Salerno, G., Randazzo, D., 2009. $SO_2$ flux from
566 Stromboli during the 2007 eruption: Results from the FLAME network and traverse
567 measurements. J. Volcanol. Geotherm. Res. 182 (3-4), 214-220.
568 Burton, M., Sawyer, G., Granieri, D., 2013. Deep carbon emissions from volcanoes. Rev.
569 Mineral. Geochem. 75, 323-354.

570 Calvari S., Bonaccorso, A., Madonia, P., Neri, M., Liuzzo, M., Salerno, G.G., Behnke, B.,
571 Caltabiano, T., Cristaldi, A., Giuffrida, G., La Spina, A., Marotta, E., Ricci, T.,
572 Spampinato, L., 2014. Major eruptive style changes induced by structural modifications of
573 a shallow conduit system: the 2007-2012 Stromboli case. Bull. Volcanol. 76, 841. doi:
574 10.1007/s00445-014-0841-7.
575 Capasso, G., Carapezza, M.L., Federico, C., Inguaggiato, S., Rizzo, A., 2005. Geochemical
576 monitoring of the 2002–2003 eruption at Stromboli volcano (Italy): precursory changes in
577 the carbon and helium isotopic composition of fumarole gases and thermal waters. Bull.
578 Volcanol. 68, 118–134. doi: 10.1007/s00445-005-0427-5.
579 Carapezza, M.L., Federico, C. 2000. The contribution of fluid geochemistry to the volcano
580 monitoring of Stromboli. J. Volcanol. Geotherm. Res. 95 (1–4), 227–245. doi:
581 10.1016/S0377-0273(99)00128-6.
582 Carapezza, M.L., and D. Granieri (2004). CO2 soil flux at Vulcano (Italy): comparison of active
583 and passive methods and application to the identification of actively degassing structure,
584 Appl. Geochem. 19, 73-88.
585 Carapezza, M.L., Inguaggiato, S., Brusca, L., Longo, M. 2004. Geochemical precursors of the
586 activity of an open-conduit volcano: The Stromboli 2002-2003 eruptive events. Geophys.
587 Res. Lett. 31 (7), L07620. doi: 10.1029/2004GL019614.
588 Carapezza, M.L., Ricci, T., Ranaldi, M., Tarchini, L., 2009. Active degassing structures of
589 Stromboli and variations in diffuse $CO_2$ output related to the volcanic activity. J. Volcanol.
590 Geotherm. Res. 182 (3–4), 231–245.
591 Carapezza, M.L., Cigolini C., Coppola D., Laiolo M., Ranaldi, M., Ricci T., Tarchini, L., 2010.
592 The role played by the environmental factors on diffuse soil degassing at Stromboli

volcano. IAVCEI – Cities on Volcanoes 6th, CoV6/1.3/P/47, Tenerife, Canary Islands, Spain.

Chouet, B., Saccorotti, G., Martini, M., Dawson, P., De Luca, G., Milana, G., Scarpa, R., 1997. Source and path effects in the wavefields of tremor and explosions at Stromboli Volcano, Italy. J. Geophys. Res. 102, 15,129 – 15,150.

Cigolini, C., Salierno, G., Gervino, G., Bergese, P., Marino, C., Russo, M., Prati, P., Ariola, V., Bonetti, R., Begnini, S., 2001. High-resolution Radon Monitoring and Hydrodynamics at Mount Vesuvius. Geophys. Res. Lett. 28 (21), 4035-4039.

Cigolini, C., Gervino, G., Bonetti, R., Conte, F., Laiolo, M., Coppola, D., Manzoni, A., 2005. Tracking precursors and degassing by radon monitoring during major eruptions at Stromboli Volcano (Aeolian Islands, Italy). Geophys. Res. Lett. 32, L12308. doi: 10.1029/2005GL022606.

Cigolini, C., Laiolo, M., Coppola, D., 2007. Earthquake-volcano interactions detected from radon degassing at Stromboli (Italy). Earth Planet. Sci. Lett. 257, 511-525.

Cigolini, C., Laiolo, M., Bertolino, S., 2008. Probing Stromboli volcano from the mantle to paroxysmal eruptions. In: Zellmer, G., Hammer, J., (Eds.), Dynamics of Crustal Magma Transfer, Storage, and Differentiation – integrating geochemical and geophysical constraints. Geological Society, London, Special Publication, 304, pp. 33-70.

Cigolini C. Poggi, P., Ripepe, M., Laiolo M., Ciamberlini C., Delle Donne, D., Ulivieri, G., Coppola D., Lacanna, G., Marchetti, E., Piscopo, D., Genco, R., 2009. Radon surveys and real-time monitoring at Stromboli volcano: Influence of soil temperature, atmospheric

615 pressure and tidal forces on $^{222}$Rn degassing. J. Volcanol. Geotherm. Res. 184 (3-4), 381-
616 388.
617 Cigolini C., Laiolo, M., Ulivieri, G., Coppola, D., Ripepe, M., 2013. Radon mapping, automatic
618 measurements and extremely high $^{222}$Rn emissions during the 2002–2007 eruptive
619 scenarios at Stromboli volcano. J. Volcanol. Geotherm. Res. 264, 49- 65.
620 Cigolini, C., Laiolo, M., Coppola, D., 2014. Revisiting the last major eruptions at Stromboli
621 volcano: inferences on the role of volatiles during magma storage and decompression. In:
622 Zellmer, G.F., Edmonds, M., Straub, S.M. (Eds.), The Role of Volatiles in the Genesis,
623 Evolution and Eruption of Arc Magmas. Geological Society, London, Special Publication,
624 304, pp. 33-70.
625 Coppola, D., Piscopo, D., Laiolo, M., Cigolini, C., Delle Donne, D., Ripepe, M., 2012. Radiative
626 heat power at Stromboli volcano during 2000-2011: twelve years of MODIS observations.
627 J. Volcanol. Geotherm. Res. 215-216, 48-60, doi: 10.1016/j.jvolgeores.2011.12.001.
628 Corazzato, C., Francalanci, L., Menna, M., Petrone, C.M., Renzulli, A., Tibaldi, A., Vezzoli, L.,
629 2008. What controls sheet intrusion in volcanoes? Structure and petrology of the Stromboli
630 sheet complex, Italy. J. Volcanol. Geotherm. Res. 173 (1-2), 26-54.
631 De Gregorio, S., Camarda, M., Gurrieri, S., Favara, R., 2014. Change in magma supply
632 dynamics identified in observations of soil $CO_2$ emissions in the summit area of Mt. Etna.
633 Bull. Volcanol.76 (8), 1-8. doi: 10.1007/s00445-014-0846-2.
634 Faber, E., Morán, C., Poggenburg, J., Garzón, G., Teschner, M., 2003. Continuous gas
635 monitoring at Galeras Volcano, Colombia: First evidence. J. Volcanol. Geotherm. Res.,
636 125 (1-2), 13-23.

637 Federico, C., Brusca, L., Carapezza, M.L., Cigolini, C., Inguaggiato, S., Rizzo, A., Rouwet, D.,
638 2008. Geochemical prediction of the 2002–2003 Stromboli eruption from variations in $CO_2$
639 and $^{222}Rn$ emissions and in Helium and Carbon isotopes. In: Calvari, S., Inguaggiato, S.,
640 Ripepe, M. & Rosi, M. (Eds.), The Stromboli volcano: an integrated study of the 2002–
641 2003 eruption. AGU, Geophysical Monograph Series, Washington D.C. 182, pp. 117-128.
642 Finizola, A., Sortino, F., Lenat, J.F., Valenza, M., 2002. Fluid circulation at Stromboli volcano
643 (Aeolian Islands, Italy) from self-potential and $CO_2$ surveys. J. Volcanol. Geotherm. Res.
644 116, 1-18.
645 Finizola, A., Sortino, F., Lénat, J.F., Aubert, M., Ripepe, M., Valenza, M., 2003. The summit
646 hydrothermal system of Stromboli. New insights from self-potential, temperature, $CO_2$ and
647 fumarolic fluid measurements, with structural and monitoring implications. Bull. Volcanol.
648 65, 486–504.
649 Finizola, A., Revil, A., Rizzo, E., Piscitelli, S., Ricci, T., Morin, J., Angeletti, B., Mocochain, L.,
650 Sortino, F., 2006. Hydrogeological insights at Stromboli volcano (Italy) from geoelectrical,
651 temperature, and $CO_2$ soil degassing investigations. Geophys. Res. Lett. 33 (17), L17304.
652 Finizola, A., Aubert, M., Revil, A., Schütze, C., Sortino, F., 2009. Importance of structural
653 history in the summit area of Stromboli during the 2002–2003 eruptive crisis inferred from
654 temperature, soil $CO_2$, self-potential, and electrical resistivity tomography. J. Volcanol.
655 Geotherm. Res. 183 (3–4), 213–227.
656 Francalanci, L, Manetti, P, Peccerillo, A., 1989. Volcanological and magmatological evolution
657 of Stromboli volcano (Aeolian Islands): the roles of fractional crystallisation, magma
658 mixing, crustal contamination and source heterogeneity. Bull. Volcanol. 51, 355-378

Francalanci, L., Tommasini, S., Conticelli, S., 2004. The volcanic activity of Stromboli in the 1906-1998 AD period: Mineralogical, geochemical and isotope data relevant to the understanding of the plumbing system. J. Volcanol. Geotherm. Res. 131 (1-2), 179-211.

Gauthier, P.J., Condomines, C., 1999. $^{210}Pb$–$^{226}Ra$ radioactive disequilibria in recent lavas and radon degassing: inferences on the magma chamber dynamics at Stromboli and Merapi volcanoes. Earth Planet. Sci. Lett. 172, 111–126.

Giammanco, S., Sims, K.W., Neri, M., 2007. Measurements of $^{220}Rn$ and $^{222}Rn$ and $CO_2$ emissions in soil and fumarole gases on Mt. Etna Volcano (Italy): implications for gas transport and shallow ground fracture. Geochem. Geophys. Geosyst. 8, Q10001. doi: 10.1029/2007GC001644.

Girault, F., Perrier, F., 2012. Estimating the importance of factors influencing the radon-222 flux from building walls. Sci. Tot. Environm. 433, 247-263.

Girault, F., Perrier, F., 2014. The Syabru-Bensi hydrothermal system in central Nepal: 2. Modeling and significance of the radon signature, J. Geophys. Res. 119, 4056-4089.

Girault, F., Perrier, F., Crockett, R., Bhattarai, M.,Koirala, B.P., France-Lanord, C., Agrinier, P., Ader, M., Fluteau, F., Gréau, C., Moreira, M., 2014. The Syabru-Bensi hydrothermal system in central Nepal: 1. Characterization of carbon dioxide and radon fluxes. J. Geophys. Res. 119, 4017-4055.

Granieri, D., Chiodini, G., Marzocchi, W., Avino, R., 2003. Continuous monitoring of CO2 soil diffuse degassing at Phlegraean Fields (Italy): influence of environmental and volcanic parameters, Earth Planet. Sci. Lett. 212, 167-179.

Gründel, M., Postendörfer. J., 2003. Characterization of an electronic Radon gas personal Dosimeter. Rad. Prot. Dosim. 107 ( 4), 287–292.

682 Hayashi, K., Yasuoka, Y., Nagahama, H., Muto, J., Ishikawa, T., Omori, Y., Suzuki, T., Homma,
683 Y., Mukai, T., 2015. Normal seasonal variations for atmospheric radon concentration: a
684 sinusoidal model..J Environ Radioact. 53, 139:149. doi: 10.1016/j.jenvrad.2014.10.007.
685 Hernandez, P., Perez, N., Salazar, J., Reimer, M., Notsu, K., Wakita, H., 2004. Radon and
686 helium in soil gases at Cañadas caldera, Tenerife, Canary Islands, Spain. J. Volcanol.
687 Geotherm. Res. 131, 59-76.
688 Hornig-Kjarsgaard., I., Keller., J., Koberski, U., Stadbauer, E., Francalanci, L., Lenhart, R.,
689 1993. Geology, stratigraphy and volcanological evolution of the island of Stromboli,
690 Aeolian arc, Italy. Acta Vulcanol. 3, 21– 68.
691 Inguaggiato, S., Jácome Paz, M.P., Mazot, A., DelgadoGranados, H., Inguaggiato, C., Vita, F.
692 2013. $CO_2$ output discharged from Stromboli Island (Italy). Chem. Geol. 339, 52-60.
693 Kotrappa, P., Dempsey, J.C., Stieff, L.R., 1993. Recent advances in electret ion chamber
694 technology. Radiat. Protect. Dosim. 47, 461-464.
695 Laiolo, M., Cigolini, C., Coppola, D., Piscopo, D., 2012. Developments in real-time radon
696 monitoring at Stromboli volcano. J. Environm. Radioact. 105, 21-29.
697 Madonia, P., Fiordilino, E., 2013. Time variability of low-temperature fumaroles at Stromboli
698 island (Italy) and its application to volcano monitoring. Bull. Volcanol. 75, 776. doi:
699 10.1007/s00445-013-0776-4.
700 Makario Londoño, J., 2009. Radon and $CO_2$ emissions in different geological environments as a
701 tool for monitoring volcanic and seismic activity in central part of Colombia. Boletin de
702 Geologia, 31(2), 83-95.

703 Marchetti, E., Ripepe, M., 2005. Stability of the seismic source during effusive and explosive
704 activity at Stromboli Volcano. Geophys. Res. Lett. 32 (3), 1–5.
705 doi:10.1029/2004GL021406.
706 Martin-Luis, M.C., Steinitz, G., Soler, V., Quesada, M.L., Casillas, R. 2015. $^{222}Rn$ and $CO_2$ at
707 Las Cañadas Caldera (Tenerife, Canary Islands). Eur. Phys. J. Special Topics 224 (4), 641-
708 657.
709 Métrich, N., Bertagnini, A., Landi, P., Rosi, M., 2005. Triggering mechanism at the origin of
710 paroxysm at Stromboli (Aeolian Archipelago, Italy): The 5 April 2003 eruption. Geophys.
711 Res. Lett. 32, L10305. doi: 10.10129/2004GL022257.
712 Métrich, N.A., Bertagnini, A. & Di Muro, A. 2010. Conditions of Magma Storage, Degassing
713 and Ascent at Stromboli: New Insights into the Volcano Plumbing System with Inferences
714 on the Eruptive Dynamics. J. Petrol. 51, 603-626.
715 Mogro-Campero, A., Fleischer, R.L., 1977. Subterrestrial fluid convection: a hypothesis for long
716 distance migration of radon within the earth. Earth Planet. Sci. Lett. 34, 321-325.
717 Nazaroff, W.W., 1992. Radon transport from soil to air. Rev. Geophys. 30, 137-160. doi:
718 10.1029/92RG00055.
719 Padilla, G.D., Hernández, P.A., Padrõn, E., Barrancos, J., Pérez, N.M., Melián, G., Nolasco,
720 D., Dionis, S., Rodríguez, F., Calvo, D., Hernández, I., 2013. Soil gas radon emissions
721 and volcanic activity at El Hierro (Canary Islands): The 2011-2012 submarine eruption.
722 Geochem. Geophys. Geosyst., 14 (2), 432-447.
723 Padilla, G.D., Hernandez, P.A., Pérez, N.M., Pereda, E., Padron, E., Melian, G., Barrancos, J.,
724 Rodriguez, F., Dionis, S., Calvo, D., Herrera, M., Strauch, W., Munoz, A., 2014.
725 Anomalous diffuse $CO_2$ emissions at the Masaya volcano (Nicaragua) related to seismic-

726 volcano unrest. Pure Appl. Geophys. 171 (8), 1791-1804. doi: 10.1007/s00024-013-0756-
727 9.
728 Padrón, E., Padilla, G., Hernández, P.A., Pérez, N.M., Calvo, D., Nolasco, D., Barrancos, J.,
729 Melián, G.V., Dionis, S., Rodríguez, F., 2013. Soil gas geochemistry in relation to eruptive
730 fissures on Timanfaya volcano, Lanzarote Island (Canary Islands, Spain). J. Volcanol.
731 Geotherm. Res. 250, 91–99.
732 Pan, V., Holloway, J.R., Hervig, R.L., 1991. The pressure and temperature dependence of carbon
733 dioxide solubility in tholeiitic basalt melts. Geochim. Cosmochim. Acta 55, 1587–1595.
734 Papachristodoulou, C., Ioannides, K., Spathis, S. (2007). The effect of moisture content on
735 radon diffusion through soil: Assessment in laboratory and field experiments. Health Phys
736 92 (3), 257-264.
737 Papale, P., Moretti, R., Barbato, D., 2006. The compositional dependence of the multicomponent
738 volatile saturation surface in silicate melts. Chem. Geol. 229, 78–95.
739 Pérez, N.M., Hernández, P.A., Padrón, E., Melián, G., Marrero, R., Padilla, G., Barrancos, J.,
740 Nolasco, D., 2007. Precursory subsurface $^{222}$Rn and $^{220}$Rn degassing signatures of the 2004
741 seismic crisis at Tenerife, Canary Islands. Pure Appl. Geophys. 164, 2431-:2448, doi:
742 10.1007/s00024-007-0280.
743 Perrier, F., Girault, F., 2012. Harmonic response of soil radon-222 flux and concentration
744 induced by barometric oscillations. Geophys..J. Int. , doi: 10.1093/gji/ggt280.
745 Perrier, F., Richon, P., Sabroux, J.C., 2009. Temporal variations of radon concentration in the
746 saturated soil of Alpine grassland: The role of groundwater flow. Sci. Tot. Environm. 407,
747 2361-2371.

748 Pinault, J.L., Baubron, J.C., 1996. Signal processing of soil gas radon, atmospheric pressure and
749 soil temperature data: a new approach for radon concentration modelling. J. Geophys. Res.
750 B: Solid Earth 101 (2), 3157-3171.
751 Revil, A., Finizola, A., Ricci, T., Delcher, E., Peltier, A., Barde-Cabusson, S., Avard, G., Bailly,
752 T.,Bennati, L., Byrdina, S., Colonge, J., Di Gangi, F., Douillet, G., Lupi, M., Letort, J.,
753 Tsang Hin Sun, E., 2011. Hydrogeology of Stromboli volcano, Aeolian Islands (Italy) from
754 the interpretation of resistivity tomograms, self-potential, soil temperature and soil $CO_2$
755 concentration measurements. Geophys. J. Int. 186 (3), 1078-1094.
756 Rinaldi, A.P., Vandemeulebrouck, J., Todesco, M., Viveiros, F. 2012. Effects of atmospheric
757 conditions on surface diffuse degassing. J. Geophys. Res. Solid Earth 117, B11201. doi:
758 10.1029/2012JB009490.
759 Ripepe, M., Delle Donne, D., Lacanna, G., Marchetti, E. and Ulivieri, G., 2009. The onset of the
760 2007 Stromboli effusive eruption recorded by an integrated geophysical network. J.
761 Volcanol. Geotherm. Res. 182(3-4): 131-136.
762 Rizzo, A., Grassa, F., Inguaggiato, S., Liotta, M., Longo, M., Madonia, P., Brusca, L., Capasso,
763 G., Moricia, S., Rouwet, D., Vita, F., 2009. Geochemical evaluation of observed changes
764 in volcanic activity during the 2007 eruption at Stromboli (Italy). J. Volcanol. Geotherm.
765 Res. 182 (3-4), 246-254.
766 Rizzo, A.L., Federico, C., Inguaggiato, S., Sollami, A., Tantillo, M., Vita, F., Bellomo, S.,
767 Longo, M., Grassa, F., Liuzzo, M., 2014. The 2014 effusive eruption at Stromboli volcano
768 (Italy): Inferences from soil $CO_2$ flux and $^3He/^4He$ ratio in thermal waters. Geophys. Res.
769 Lett. 42, doi: 10.1002/2014GL062955.

770 Rosi, M., Bertagnini, A., Landi, P., 2000. Onset of persisting activity at Stromboli Volcano
771 (Italy). Bull. Volcanol. 62, 294-300.
772 Sakoda, A., Ishimori, Y., Hanamoto, K., Kataoka, T., Kawabe, A., Yamaoka, K., 2010.
773 Experimental and modeling studies of grain size and moisture content effects on radon
774 emanation. Radiat. Measurem. 45, 204-210.
775 Salazar, J.M.L., Hernández, P.A., Pérez, N.M., Melián, G., Álvarez, J., Segura, F., Notsu, K.,
776 2001. Diffuse emission of carbon dioxide from Cerro Negro volcano, Nicaragua, Central
777 America. Geophys. Res. Lett. 28 (22), 4275-4278.
778 Silva, C., Ferreira, T., Viveiros, F., Allard P., 2015. Soil radon ($^{222}$Rn) monitoring at Furnas
779 Volcano (São Miguel, Azores): Applications and challenges. Eur. Phys. J. Special Topics
780 224 (4), 659-686. doi: 10.1140/epjst/e2015-02398-6.
781 Siniscalchi, A., Tripaldi, S., Neri, M., Giammanco, S., Piscitelli, S., Balasco, M., Behncke, B.,
782 Magri, C., Naudet, V., Rizzo, E., 2010. Insights into fluid circulation across the Pernicana
783 Fault (Mt. Etna, Italy) and implications for flank instability. J. Volcanol. Geotherm. Res.
784 193, 137-142
785 Steinitz, G., Piatibratova, O., Kotlarsky, P., 2011. Possible effect of solar tides on radon signals.
786 J. Environm. Radioact. 102 (8), 749 – 765. doi: 10.1016/j.jenvrad.2011.04.002.
787 Tibaldi, A., 2003. Influence of cone morphology on dykes, Stromboli, Italy. J. Volcanol.
788 Geotherm. Res. 126, 79–95.
789 Tibaldi, A., 2004. Major changes in volcano behaviour after a sector collapse: Insights from
790 Stromboli, Italy. Terra Nova 16 (1), 2-8.

791 Tibaldi, A., Corazzato, C., Marani, M., Gamberi, F., 2009. Subaerial-submarine evidence of
792 structures feeding magma to Stromboli Volcano, Italy, and relations with edifice flank
793 failure and creep. Tectonophys. 469 (1-4), 112-136.
794 Tinti, S., Maramai, A., Armigliato, A., Graziani, L., Manucci, A., Pagnoni, G., Zaniboni, F.,
795 2006. Observations of physical effects from tsunamis of December 30, 2002 at Stromboli
796 volcano, southern Italy. Bull. Volcanol. 68, 450–461.
797 Toutain, J. P., Baubron, J. C., 1999. Gas geochemistry and seismotectonics: a review.
798 Tectonophys. 304, 1–27.
799 Vandeginste, B.G.M., Massart, D.L., Buydens, L.M.C., De Jong, S., Lewi, P.J., Smeyers-
800 Verbeke, J., 1988. Handbook of Chemometrics and Qualimetrics: Part B. Elsevier,
801 Amsterdam.
802 Viveiros, F., Ferreira, T., Cabral Vieira, J., Silva, C., Gaspar, J.L., 2008. Environmental
803 influences on soil $CO_2$ degassing at Furnas and Fogo volcanoes (São Miguel Island,
804 Azores archipelago). J. Volcanol. Geotherm. Res. 177, 883–893.
805 Viveiros, F., Vandemeulebrouck, J., Rinaldi, A.P., Ferreira, T., Silva, C., Cruz, J.V., 2014.
806 Periodic behavior of soil CO2 emissions in diffuse degassing areas of the Azores
807 archipelago: Application to seismovolcanic monitoring. J. Geophys. Res. 119, 7578–7597.
808 doi:10.1002/2014JB011118.
809 Zimmer, M., Erzinger, J., 2003. Continuous $H_2O$, $CO_2$, $^{222}Rn$ and temperature measurements on
810 Merapi Volcano, Indonesia. 8J. Volcanol. Geotherm. Res. 125 (1-2), 25-38. doi:
811 10.1016/S0377-0273(03)00087.
812

## Figure Captions

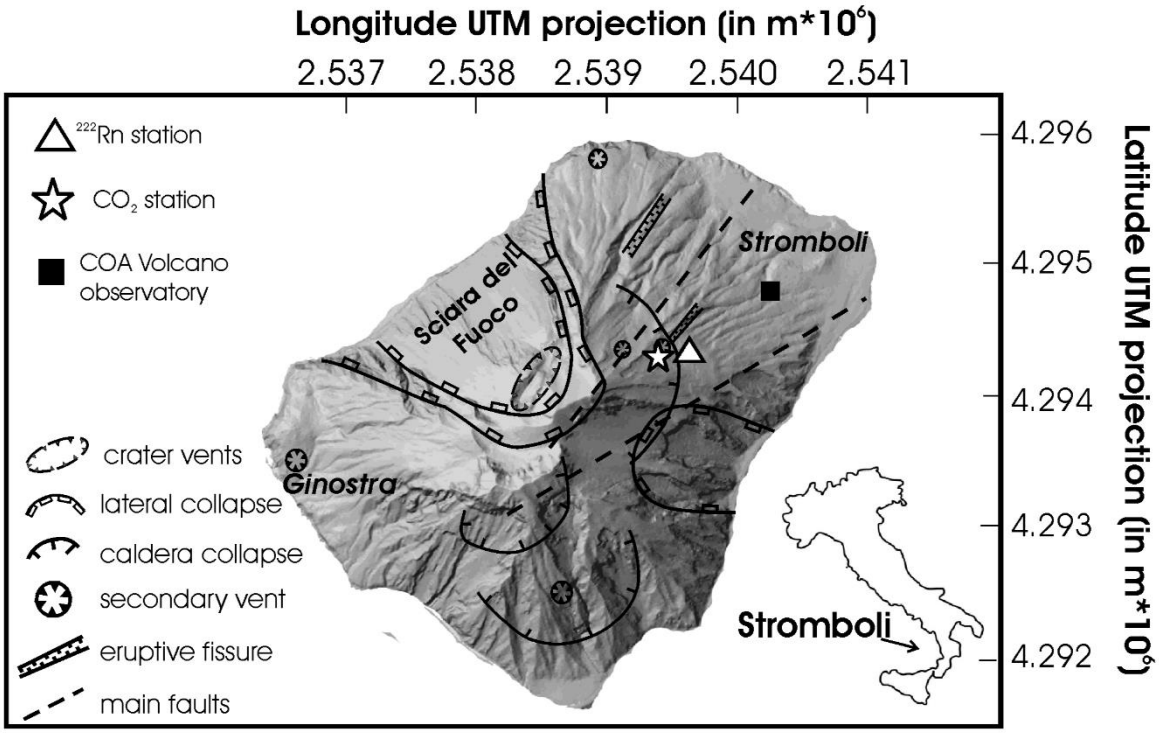


**Fig. 1.** Digital Elevation Model of Stromboli Island (from Baldi et al., 2005) with major faults and collapsed sectors (simplified from Finizola et al., 2002 and Tibaldi et al., 2009). Locations of the Volcano Observatory (COA) and of the radon and $CO_2$ flux stations are reported.

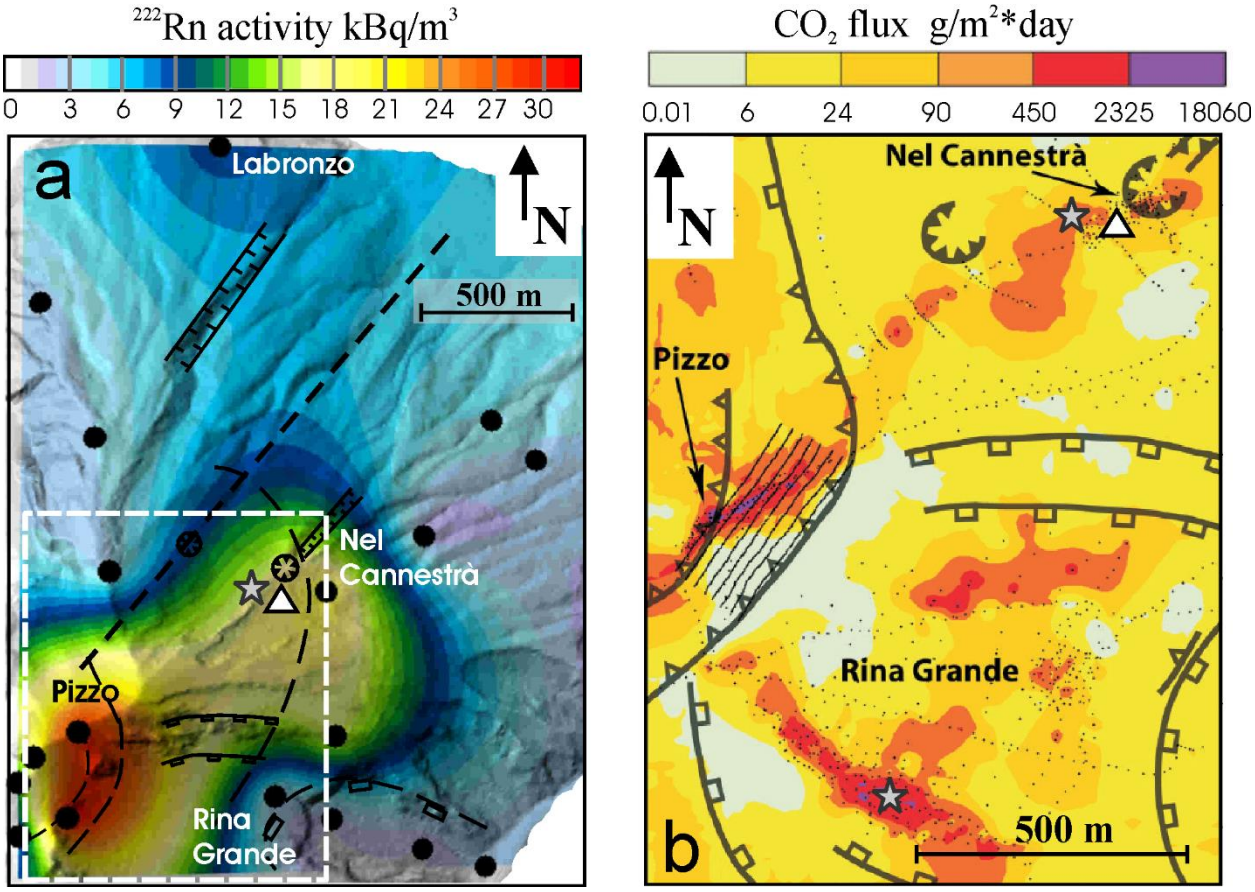


818

819 **Fig. 2** (a) Map of radon activity measured in March 10-18, 2007 on the NE flank of Stromboli. Full
820 circles indicate measurement sites; the contour lines of radon emissions have been obtained by kriging
821 (Cigolini et al., 2013). The triangle indicates the location of the $^{222}$Rn automatic station. Dotted white
822 rectangle marks the area of the soil $CO_2$ flux map of March 2007 reported in b). Stars are the sites of the
823 automatic $CO_2$ stations (Carapezza et al., 2009).

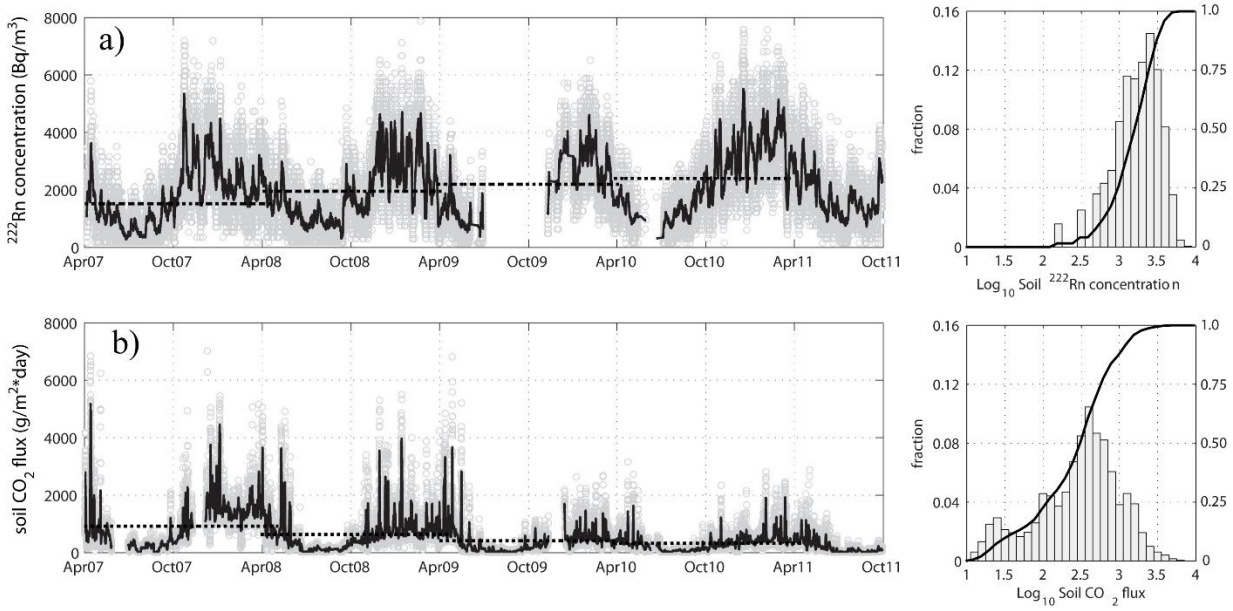


824

825 **Fig. 3.** Time-series of $^{222}$Rn activity (a) and soil $CO_2$ flux (b) recorded hourly from April 2007 to
826 September 2011 (grey dots). Black curves and the straight dotted lines represents the daily and the annual
827 average, respectively. Histograms show the multi-modal distributions.

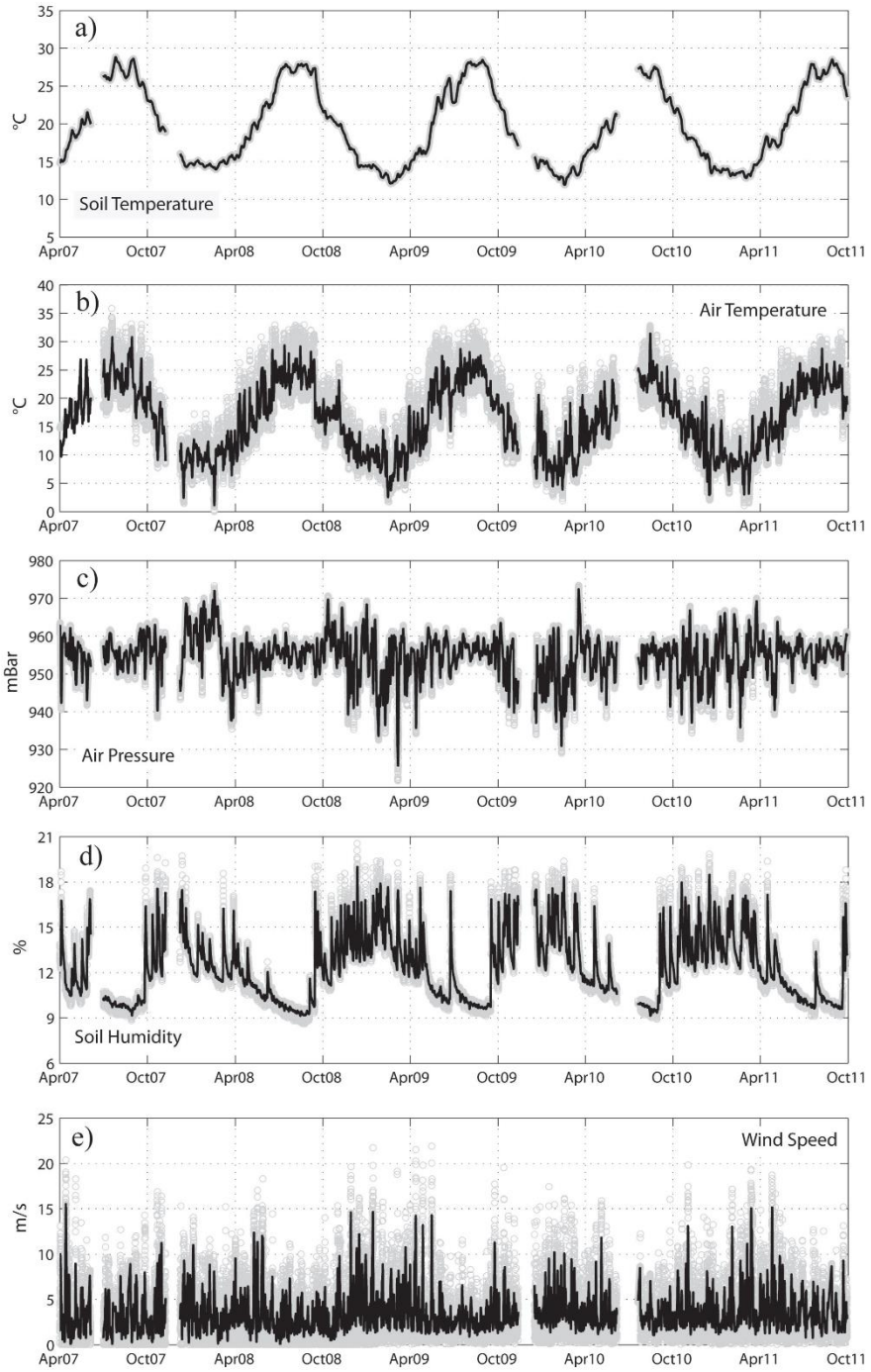


828

829 **Fig. 4.** Time-series of the main environmental parameters measured hourly from April 2007 to September

830 2011 at NC station (grey dots). Black curves are the daily average.

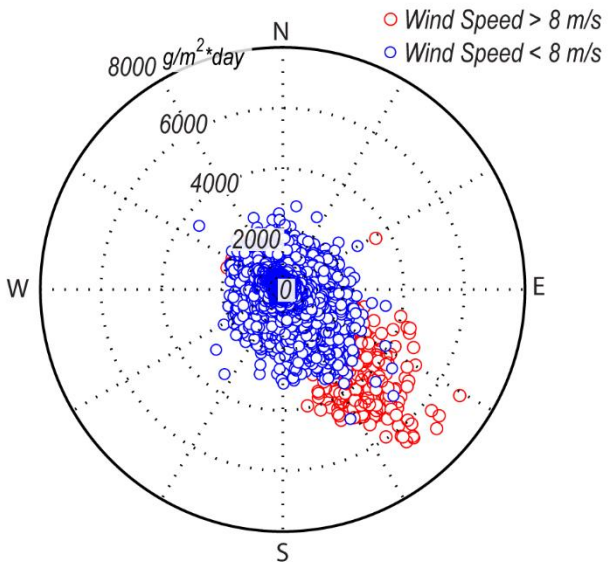


831

832

833 **Fig. 5.** Soil $CO_2$ flux vs. wind direction. Red and blue circles refer to data acquired with wind speed
834 above or below 8 m/s respectively. Note that most of the high soil $CO_2$ fluxes are recorded for wind speed
835 >8m/s in the SE sector.

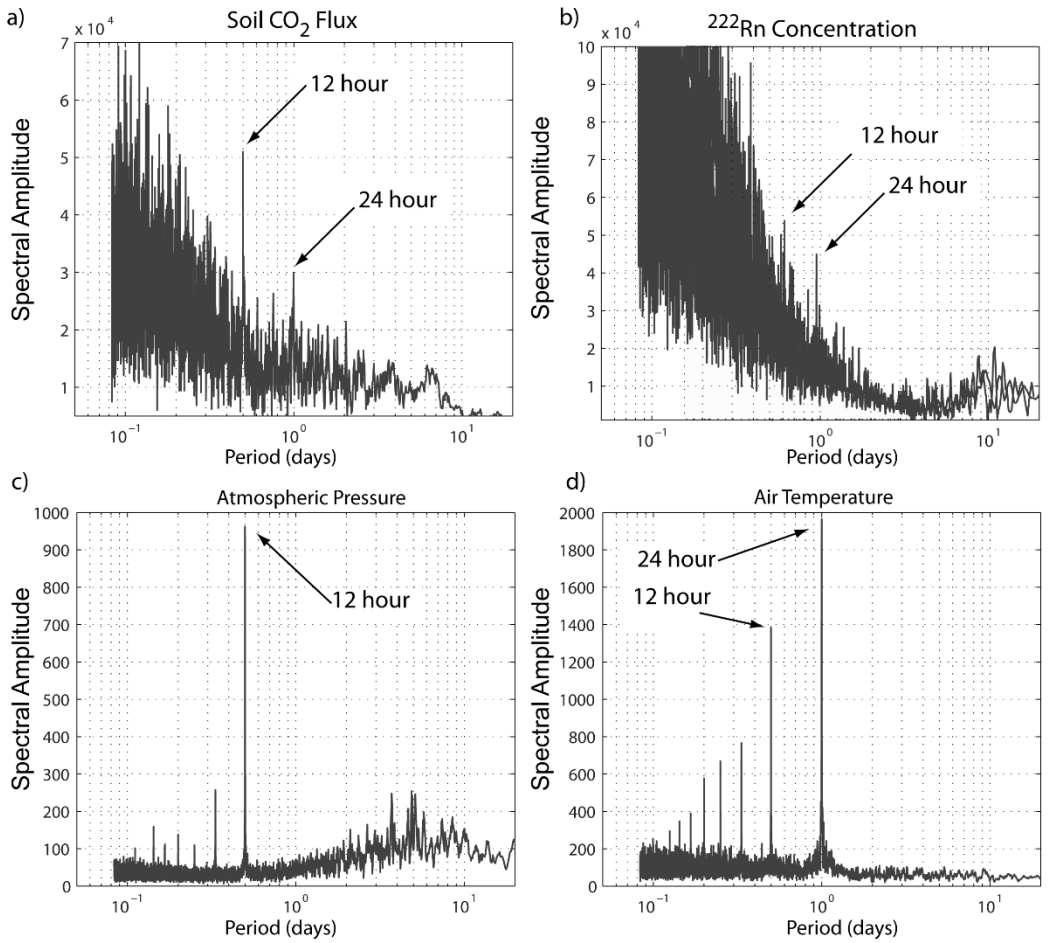


836

837 **Fig. 6.** Spectral amplitude for soil $CO_2$ flux (a), $^{222}$Rn concentration (b), atmospheric pressure (c) and air

838 temperature (d). The analyses were made over one year of hourly data (see text for details).

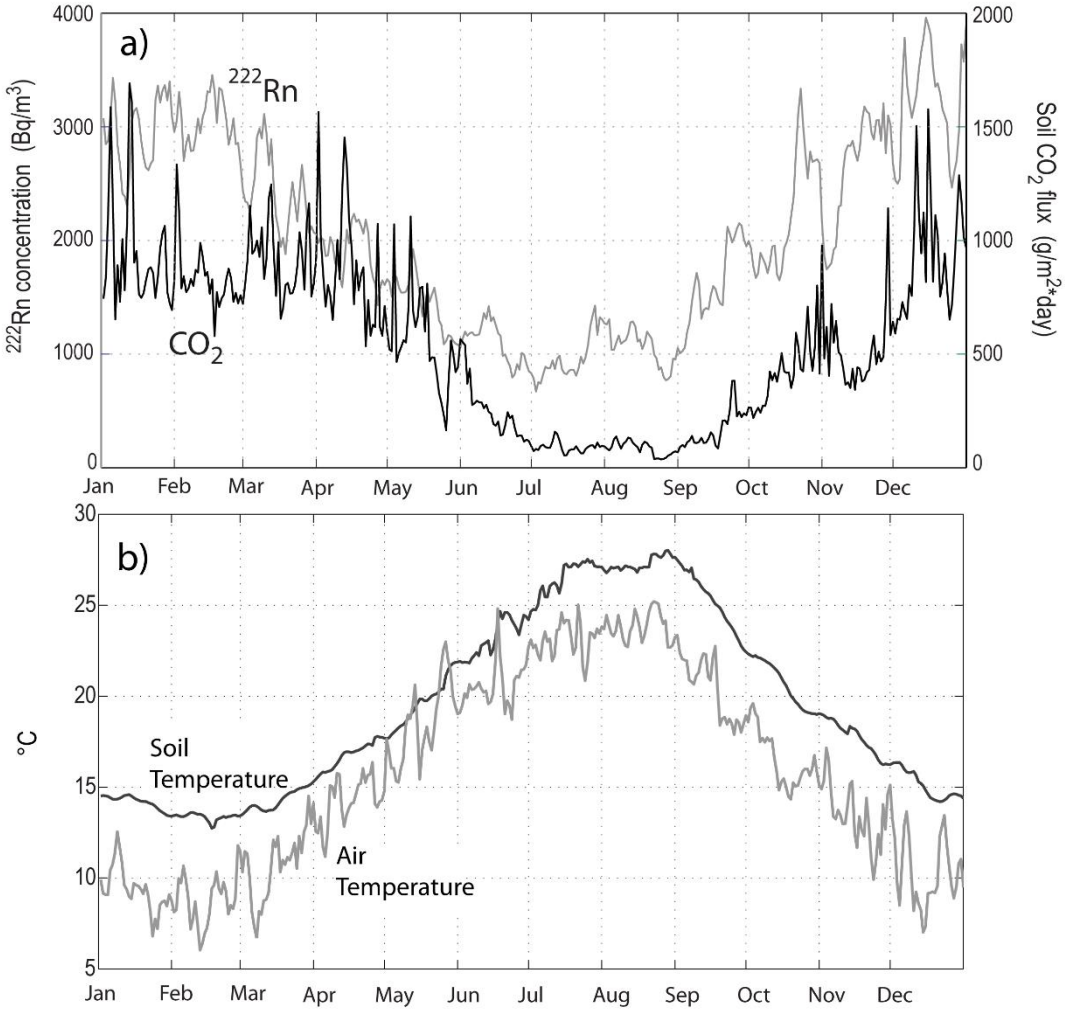


839

840 **Fig. 7.** Bulk annual trend of radon concentration and soil $CO_2$ flux (a) retrieved from the mean values
841 measured each day in the 4 years monitoring. Results are compared with the annual trend of soil and air
842 temperatures (b).

843

844

845

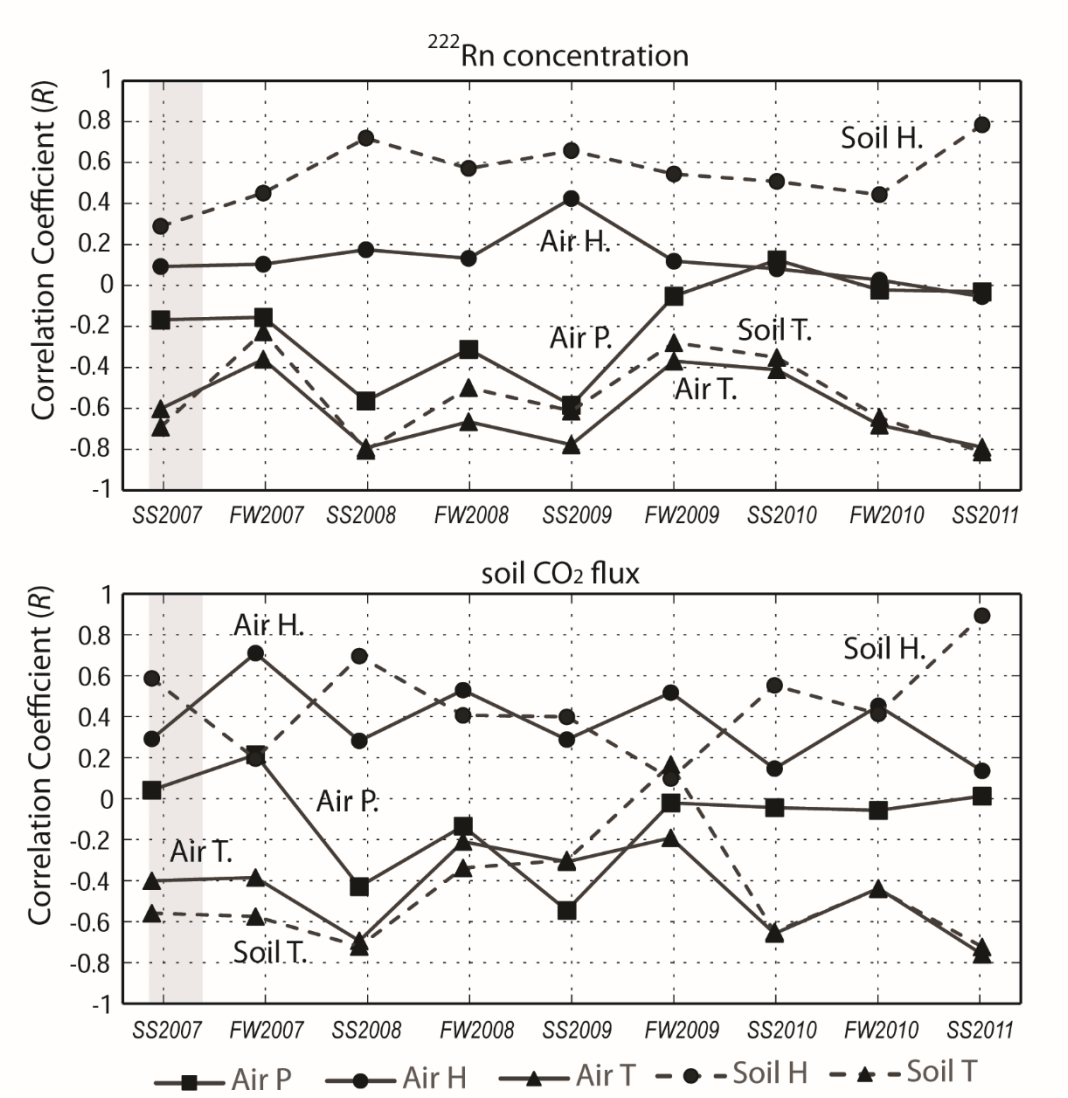


846

847 **Fig. 8.** Seasonal variations of the average correlation coefficients (R) between main atmospheric factors
848 and $^{222}$Rn concentration (above) and soil $CO_2$ flux (below). Air T: air temperature; Soil T: soil
849 temperature; Air P: barometric pressure; Soil H: soil humidity; Air H: air humidity. SS and FW refer to
850 Spring-Summer and Fall-Winter period, respectively.

851

852

853

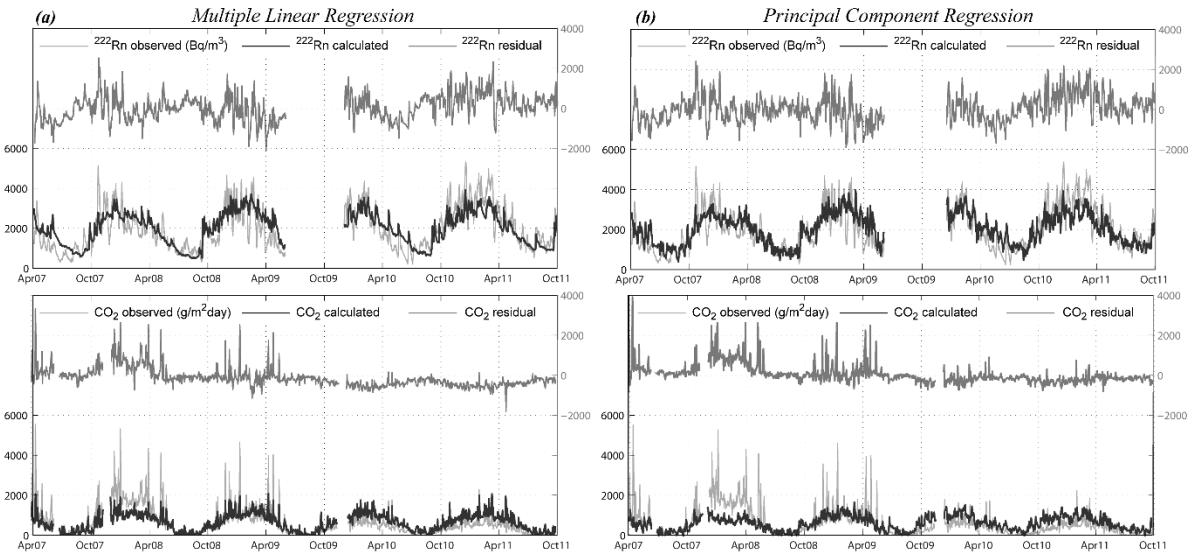


854

855 **Fig. 9.** Results from Multiple Linear Regression (a) and Principal Component Regression (b) for radon
856 activity (above) and soil $CO_2$ flux (below) during the 4 ½ years of monitoring. Data are reported as daily
857 averages. The observed, calculated and residual values are indicated.

858

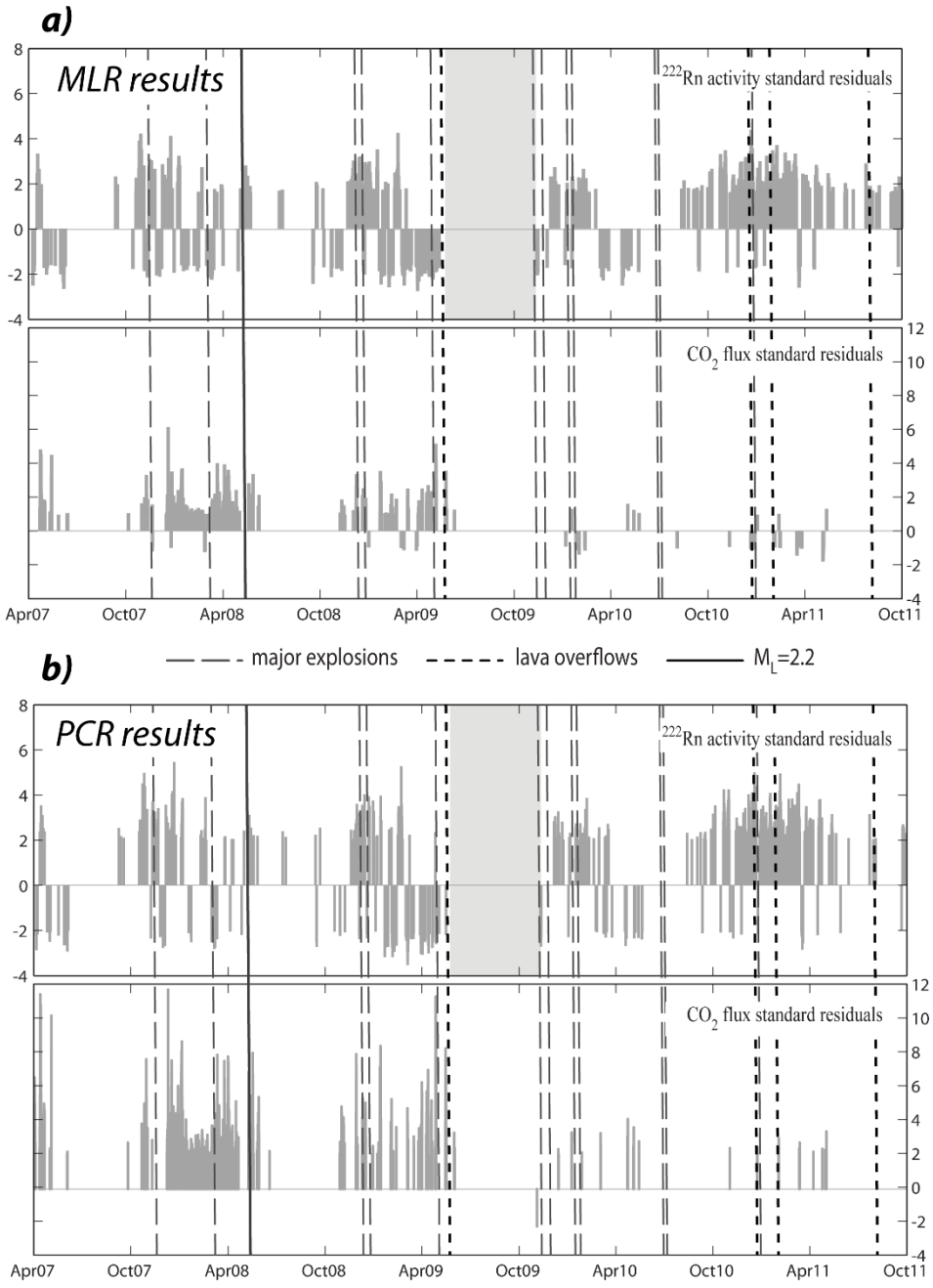


859

860 **Fig. 10.** Time series of the residuals of $^{222}$Rn concentration and soil $CO_2$ flux obtained by MLR (a) and
861 PCR (b) methods with indication of the main volcanic and seismic events occurred at Stromboli from
862 April 2007 to September 2011. Vertical axes express the standard deviation from the mean; only values ≥
863 2 σ are plotted. Grey field marks the time span when no radon data were recorded.